CLIC Note 356

The CLIC Main Linac Lattice at 1 TeV

Daniel Schulte

March 26, 1998

Abstract

This paper presents the CLIC main linac lattice at a centre-of-mass energy of 1 TeV. Its aim is to show that such a lattice is feasible resulting only in a moderate emittance growth of the transported beam due to wakefield and dispersive effects. A correction method is presented that achieves this small growth. The emittance dilution due to static and dynamic effects is discussed. Finally the multibunch effects are estimated.

Contents

1 Introduction

This paper presents the CLIC main linac lattice at a centre-of-mass energy of 1 TeV. Its aim is to show that such a lattice is feasible resulting only in a moderate emittance growth of the transported beam due to wakefield and dispersive effects. It consideres static and dynamic error sources.

Within certain limits the total luminosity $\mathcal{L}$ a linear collider can provide for a given energy consumption P_{AC} is given by $\mathcal{L} \propto \sqrt{(\delta/\epsilon_y)}\eta P_{\mathrm{AC}}$. Where η is the efficiency to turn this power into beam power, δ is the energy loss in the interaction point due to beamstrahlung and ϵ_y is the vertical emittance at the interaction point. While the allowed energy loss is limited by the experiment one has thus to increase the efficiency and decrease the vertical emittance in order to obtain high luminosity.

The emittances at the entrance of the linac are $14.7 \cdot 10^{-7}\,\mathrm{m}$ horizontally and $0.5 \cdot 10^{-7}\,\mathrm{m}$ vertically. Each bunch contains $4 \cdot 10^9$ particles and has a length of $50\,\mu\mathrm{m}$. The goal for the vertical emittance at the interaction point is less than $1.0 \cdot 10^{-7}\,\mathrm{m}$ or 100 % growth, these were the parameters presented at the LC97 workshop, where also the following was presented.

The simulations of the beamline in the following are done with a newly written program PLACET[10]. This code is based on simple tracking and therefore allows to also include nolinear effects—variations of the RF-phase, the focusing fields, the bunch charge etc. It is possible to get reasonable statistics based on a hundred machines within a few minutes depending on the correction scheme.

2 Description of the Lattice

The main linac accelerates the beam from $E_0 = 9\,\mathrm{GeV}$ to $E_f = 500\,\mathrm{GeV}$. Since in CLIC the RF power necessary to accelerate the main beam is generated by decelerating a high charge beam of low energy particles in a second beamline parallel to the main one, it is convenient to divide both lines into short modules of equal length. Therefore all components are mounted on girders with a length of 2.245 m that are connected by bellows of 3.5 cm length. Such a girder can either support four cavities with a length of 49 cm each or a quadrupole and up to three cavities depending on the quadrupole length. At the front the space necessary to hold a beam-position monitor (BPM) is foreseen. The girder layout is comparable to the one in reference [6]. The BPMs may not be necessary on the cavity girders, in which case one can save cost and space. The layout of the girders can be seen in Fig. 1.

The cavity gradient is $G = 100\,\mathrm{MV/m}$ and the maximal strength of the quadrupoles was assumed to be $125\,\mathrm{T/m}$[1].

The lattice is derived from a smooth optics, which starts with a distance between (thin) quadrupoles of $L_0 = 2.5\,\mathrm{m}$ and a focal length of $f_0 = 1.6\,\mathrm{m}$.

[1] This is a very conservative value leading to a poletip field of only 0.625 T. It was based on an actual design.

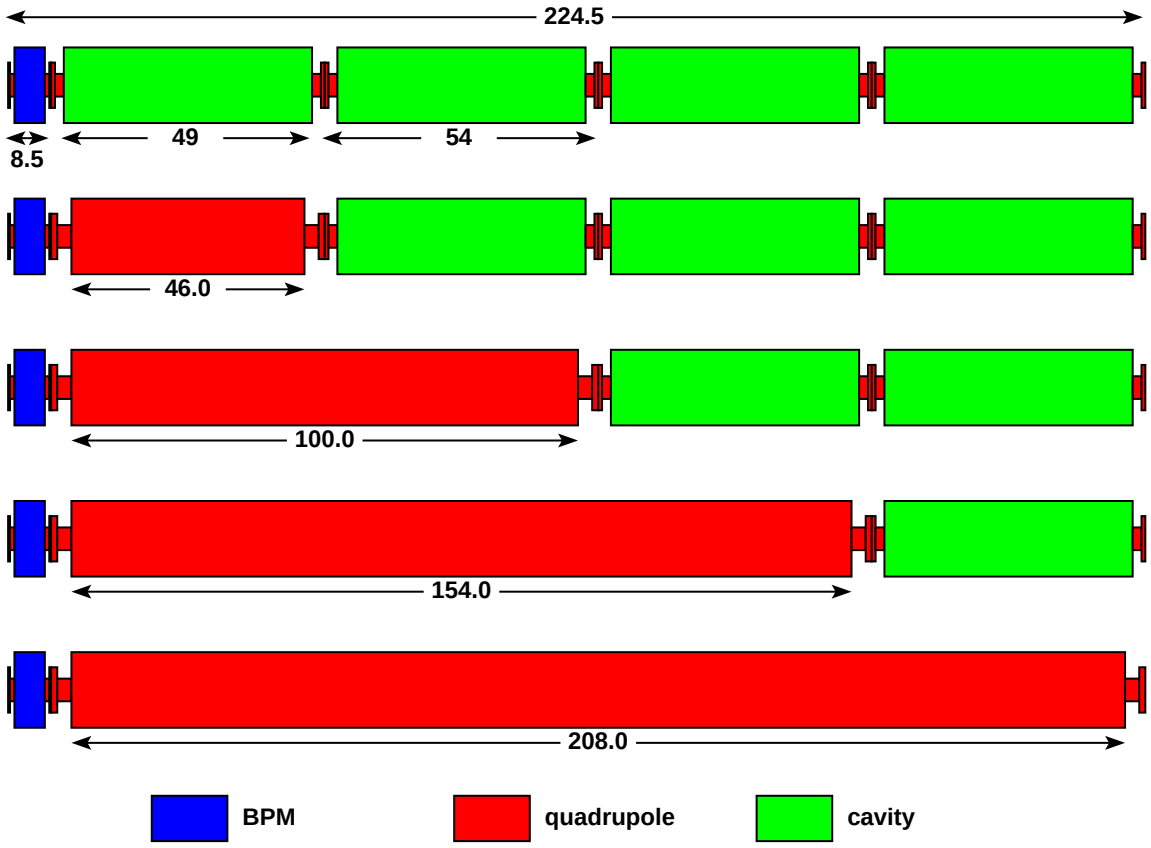

Figure 1: The layout of the girders of the main linac. All dimensions are in cm.

These values are scaled according to

$$L = L_0 \left(\frac{E}{E_0}\right)^{\alpha_L} \quad f = f_0 \left(\frac{E}{E_0}\right)^{\alpha_f} \tag{1}$$

where $\alpha_L = 0.4$ and $\alpha_f = 0.4$.

The actual lattice consists of seven sectors each with quadrupoles of equal distance, length and normalised strength. Their properties can be found in Table 1. To avoid beating of the beta-function the sectors are matched by adjusting the strength of the last three quadrupoles of each section and the first two of the following. In principle using more magnets for the matching should improve the bandwidth. The actual beta-functions and those of the scaled model can be found in Figure 2, the phase advance per cell is constantly 102.75° except for the matching regions. This is about the value that results

Sector No.	1	2	3	4	5	6	7
number of quadrupoles in sector	76	86	76	178	248	116	160
cavities replaced by quadrupole	1	1	2	2	3	3	4
length of quadrupole [m]	0.46	0.46	1.0	1.0	1.54	1.54	2.08
distance between quadrupoles [m]	2.28	4.56	4.56	6.84	9.12	11.4	11.4
cavity girders between quadrupoles	0	1	1	2	3	4	4

Table 1: Properties of the sectors of the main linac. The number of girders between quadrupoles refers to those containing only cavities.

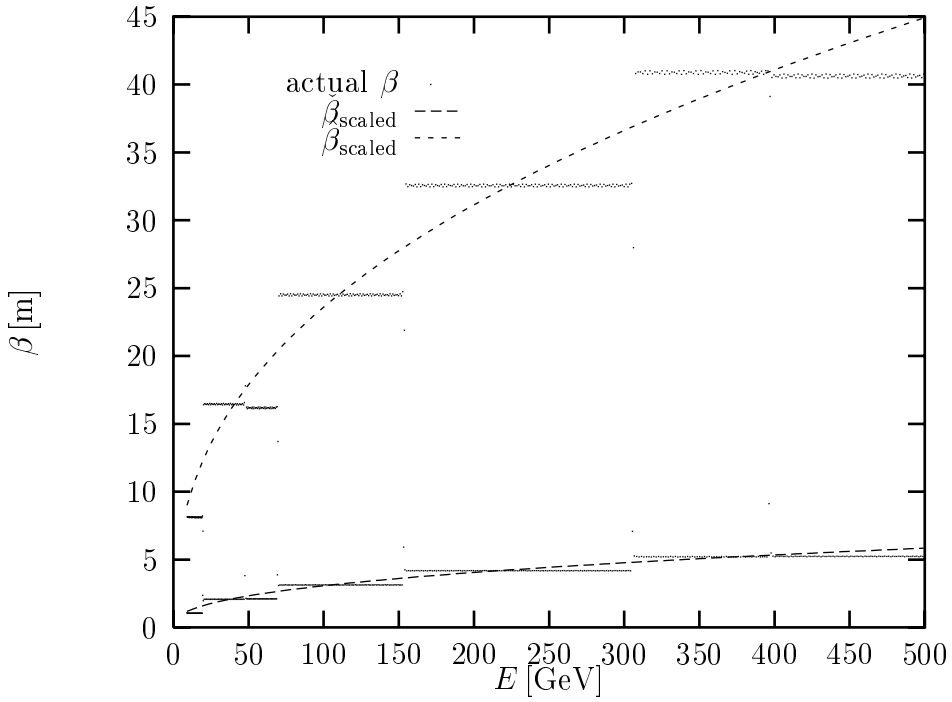

Figure 2: The beta-function of the lattice and the scaled model.

in the lowest average beta-function for a given total integrated quadrupole strength.

3 Prealignment and Wakefields

3.1 Modelling of the errors

The cavities and BPMs are mounted onto the girders with a precision of a few micrometers. The ends of consecutive girders are connected forming a chain. With the help of a system of wires they can be positioned accurately[4]. In

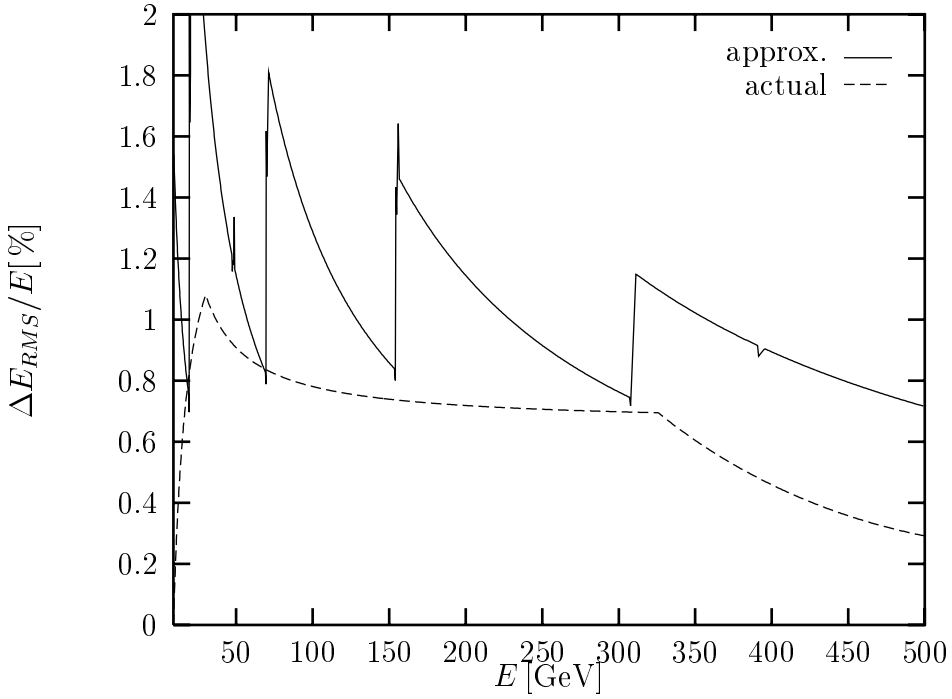

Figure 3: The RMS energy spread along the linac. The final total width is about 0.8 %.

the following it is assumed that the wavelengths of the bends introduced by this prealignment system are long compared to a betatron wavelength in the linac. In that case the emittance growth due to these bends should be small. The linac is thus modelled as a straight line with the elements scattered around the axis. All the errors are assumed to be normally distributed.

For the cavities and the BPMs a RMS position error of 10 μm is assumed. For the quadrupoles this error can be larger since besides the error of the position of the mechanical centre with respect to the reference line there can also be a difference between the mechanical and the magnetic centre. A value of 50 μm was therefore assumed.

For the correction also the BPM resolution is important. Since it is foreseen to use cavity pickups the expected resolution is better than 100 nm[12]. Also beam jitter during the correction as well as errors in the field strength of the quadrupoles may be important depending on the method used. Part of these effects can be reduced by integrating over a number of readings. These errors will be specified in the descriptions of the correction methods.

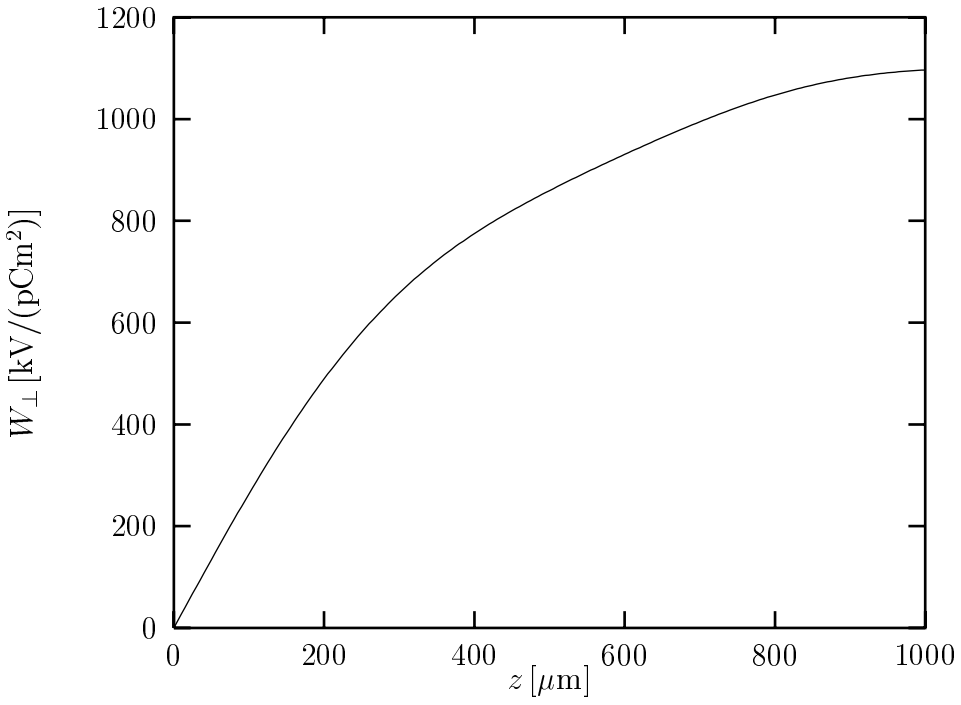

Figure 4: Transverse delta wakefields used for the simulations.

3.2 Transverse Wakefields

A particle travelling off-axis in a cavity induces a transverse dipole field which will kick the following particles. Within the same bunch this field is referred to as short range at the following bunches as longrange wakefields. The kick strength depends in reasonable approximation linearly on the offset of the inducing particle (if it is small enough) and not on the transverse position of the kicked one. It also depends strongly on the cavity—scaling approximately as [11]

$$W_\perp \propto \frac{1}{\lambda^3}\left(\frac{\lambda}{a}\right)^{2.2} \tag{2}$$

where λ is the wavelength of the RF and a the aperture. It is therefore more severe at the CLIC accelerating frequency of about 30 GHz than at 3 or 11 GHz used in the S-band and X-band designs. Considering the short range wakefields only, one can compensate this by reducing the charge and using shorter bunches. While the first reduces the amplitude of the kick the latter makes use of the fact that the transverse wakefield has a sine-like behaviour, see Fig. 4 showing the wakefield of the CLIC structure[5]. At short enough distancies behind the driving particle the wakefield thus increases linearly, so

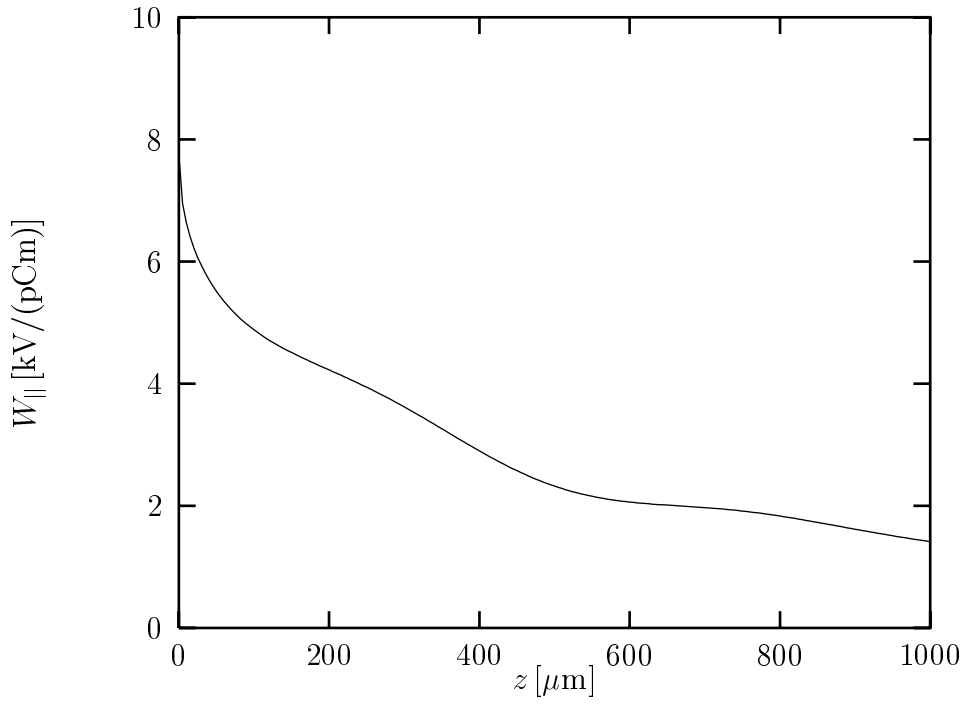

Figure 5: Longitudinal wakefield assumed for the CLIC main linac structures.

that a shorter bunch reduces the kick seen by the particles.

Several lower limits for the bunch length however exist. Among them the feasibility of producing it via bunch compression and the longitudinal beamloading that will discussed in the following.

3.3 Longitudinal Wakefields and Bunch Length

Longitudinal wakefields will induce an energy spread in the bunch such that the particles in the head have a higher energy than those in the tail. These wakefields are decreasing with distance and the one of the CLIC cavities is shown in Fig. 5[5]. Two main reasons require that the energy spread remains small, the physics requirements on the luminosity spectrum and the bandwidth of the final focus system. The latter sets a limit of about 1% full width while the former depends very much on the analysis. For a threshold scan (around top production threshold for example) it has a significant impact, while for other analysis this is less severe[2]. As a resonable

[2]Even so the average energy loss due to beamstrahlung in the interaction point will give a significant smearing of the luminosity spectrum it will keep a sharp edge at highest energies very much as the initial state radiation does. The influence of energy spread and

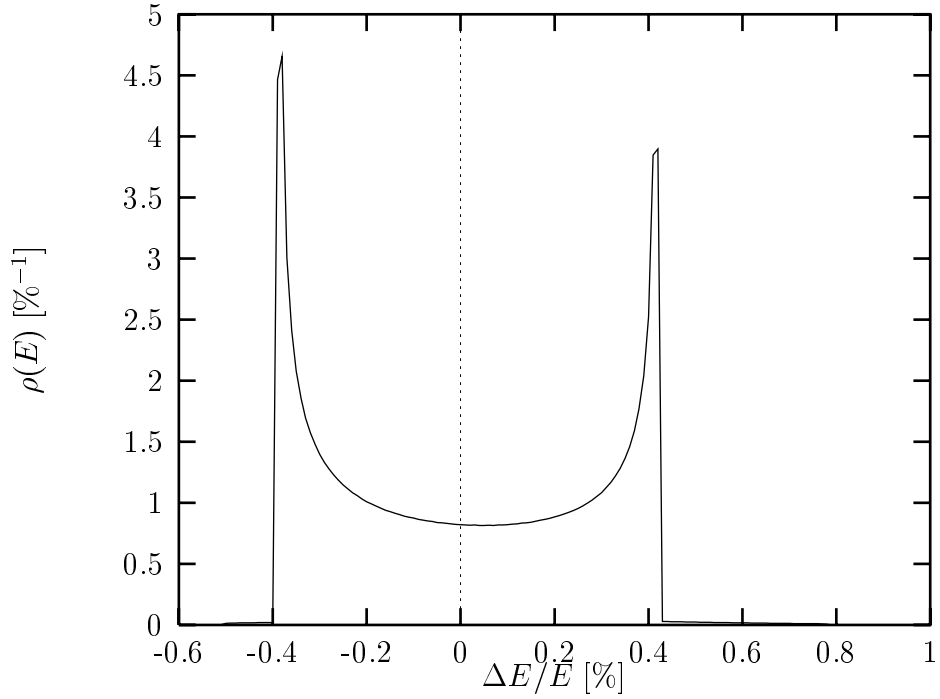

Figure 6: The energy spread at the end of the main linac.

upper limit for the full width energy spread 0.8% is adopted here in absense of a final focus design. This is the value acceptable for the NLC final focus system[8].

The energy spread induced by the wakefields depends on the bunch length, being smaller for longer bunches. It can be reduced with the help of the RF by not accelerating the bunch at full amplitude ($\Phi = 0$) but at a phase to have higher energy gain for the tail than for the head, which corresponds to a positive phase in this paper. Running off-crest leads to a slighly reduced efficiency (by a factor $\cos\Phi$). The lever arm for reducing the energy spread is given by $G\sigma_z \sin\Phi$. Allowing for a maximal average acceleration phase of $\Phi = 12^\circ$ the minimal bunch length for a given charge is fixed—for the present charge of $4 \cdot 10^9$ particles per bunch to about $50\,\mu$m

3.4 BNS-Damping

In order to reduce the wakefield effects the BNS-damping [1] has been very succesfull. The basic idea is to compensate the wakefield kick experienced by the bunch tail via stronger focusing of this tail. This can conviently be

beamstrahlung on the analysis is thus very different.

achieved introducing an energy spread in the bunch with the lower energies at the tail[3]. The required spread σ_E can be approximately calculated using [3]

$$\sigma_E \approx \frac{N r_e W_\perp(2\sigma_z) L^2}{48\gamma} \left(1 + \frac{3}{2}\cot^2\frac{\mu}{2}\right) \tag{3}$$

Here μ and l are the phase advance and length of a FODO cell and r_e is the classical electron radius. This energy spread is partly induced by the longitudinal wakefield of the bunch itself partly by accelerating in the first part of the linac with a negative phase. For the main part of the linac the RF-phase is chosen as to keep the energy spread close to the required. In the end it is necessary to reduce the energy spread to a full width of about 0.8% to be able to transport the beam through the final focus system. As an upper limit for the phase in this compensation region $\Phi = 30°$ was adopted.

Having different RF-phases along the linac reduces the efficiency further compared to using one phase only. Therefore one has to provide additional overhead, the socalled BNS-overhead. It is therefore reasonable to restrict the energy spread in the linac to not reduce the efficiency too much. Writing equation (3) in a slightly different form it is obvious that for fixed energy spread, charge and bunch length the focal length has to be adjusted[4]

$$\sigma_E \propto N W_\perp f^2 \left(1 + \frac{1}{2}\cos^2\frac{\mu}{2}\right) \tag{4}$$

In order not to let the focal length rise too much, the scaling variable $\alpha_f = 0.4$ was chosen in equation (1). To keep the total length of the quadrupoles relatively small the value $\alpha_L = \alpha_f$ was used to keep the phase advance constant. Starting from smaller values f_0 and L_0 with a scaling $\alpha_f = \alpha_L = 0.5$—such that the integrated quadrupole strength remained constant—was actually leading to comparable results. Using the same f_0 and L_0 but scaling with $\alpha_L = 0.3$ and $\alpha_f = 0.4$ as it was done before [2][6] would lead to slightly better results but an integrated quadrupole length fifty percent higher than it is now.

The acceleration phases were chosen to be $\Phi = -10°$ from 9 to 30 GeV, then $\Phi = 6°$ up to 325 GeV and finally $\Phi = 30°$ up to the end. While the energy spread is at the lower limit of the analytical prediction it is well inside a flat optimum for the different emittance dilution effects.

[3]Another option is to use RF-quadrupoles, cavities that due to their different dimensions in the two transverse planes produce a sizeable quadrupolar field. The time dependence of this field allows to apply a different kick for the head and the tail of the bunch. However it may be difficult to align these cavities precisely enough to the quadrupoles. If this can not be done the resulting emittance growth is increased drastically [2].

[4]The phase advance gives only a small correction.

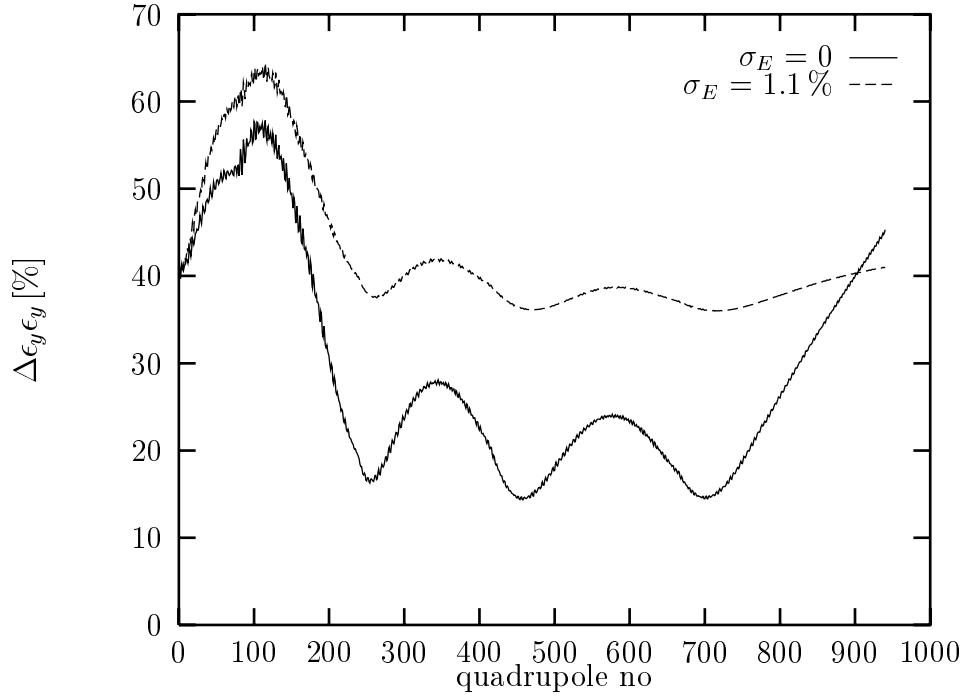

Figure 7: The vertical emittance growth for different BNS damping conditions. The beamline was perfectly aligned and the beams were offset at the entrance by $\delta y = \sigma_y$. The emittance is given with respect to the beamline axis.

4 Emittance Growth without Correction

Among the sources of emittance growth that can not be reduced with a correction scheme jitter of the beam and the quadrupoles play an important role. The roll of quadrupoles around their longitudinal axis is static and can in principle be cured. Here only the coupling of the emittances is considered for an otherwise perfect linac.

4.1 Beam Jitter

Initial offset of the beam at the linac entrance caused by jitter is a possibly import source of emittance growth. In Fig. 7 the vertical emittance growth along the linac is shown for the chosen acceleration phases. The final emittance growth with respect to the axis is about 40 % for an initial offset of σ_y.

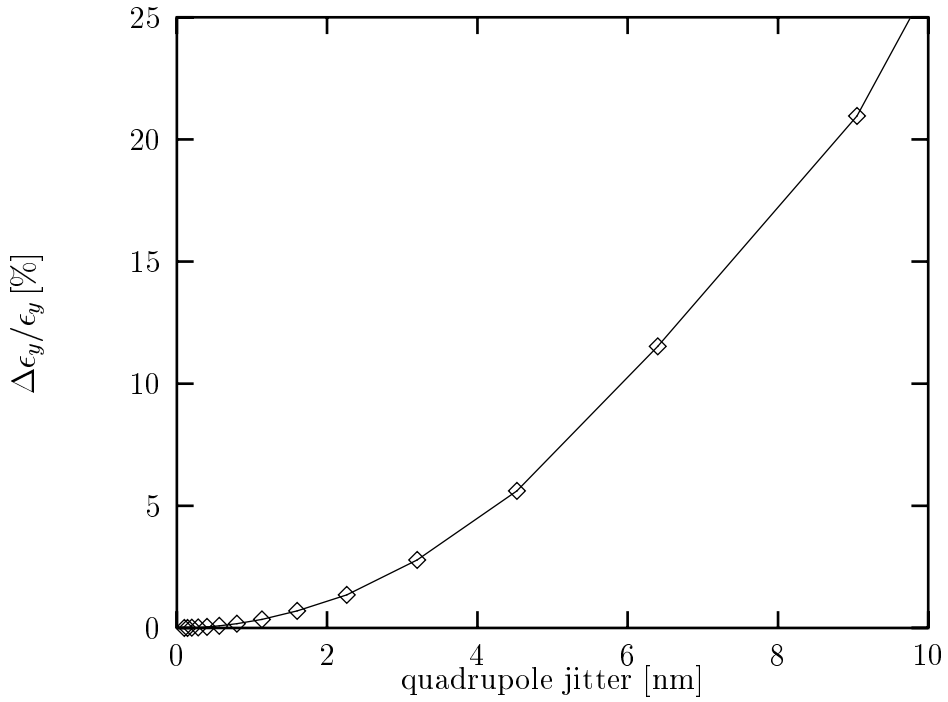

Figure 8: The emittance growth caused by quadrupole jitter.

4.2 Quadrupole Jitter

The calculation is also performed starting from a perfectly aligned linac and simulating the quadrupole jitter keeping all other elements fixed. As Fig. 8 shows the emittance increases for an RMS jitter of 4 nm about 4 % with respect to the beamline axis and is thus acceptable.

4.3 Quadrupole Roll

Angular roll of the quadrupoles around their longitudinal axis causes emittance increase through the coupling of the two planes. Since the horizontal emittance is much large than the vertical mainly the latter will affected. The coupling can be reduced by having different phase advances in the two planes, which can be achieved by using different strengths for the focusing and defocusing magnets. This was not included in the lattice design until now.

For a first overview only the emittance increase through the coupling of the two emittances is calculated not the effect on the correction itself. Figure 9 shows the dependence of the increase in vertical emittance on the quadrupole RMS roll angle. For an assumed error of $\sigma_{\text{roll}} = 300\,\mu$radian the

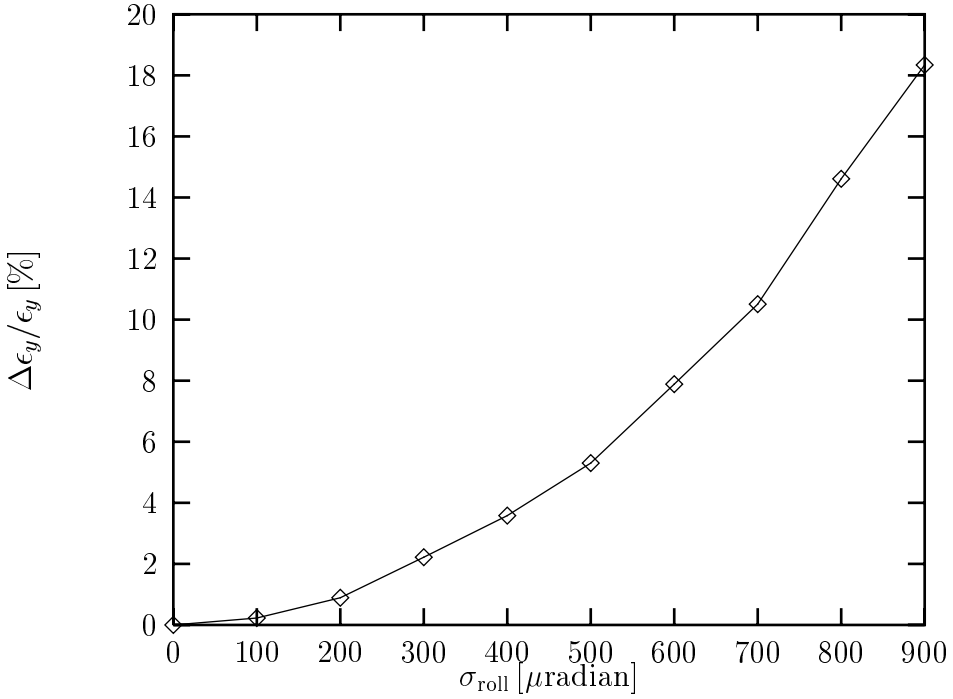

Figure 9: Dependence of the growth of the vertical emittance due to coupling of the two emittances on the RMS quadrupole roll angle

emittance growth is less than 3%.

5 Emittance Growth with Correction

Due to the large offsets of the beamline elements a correction technique has to be applied. The simplest one is the so-called one-to-one correction, a more sophisticated but still straightforward one the ballistic method.

5.1 One-To-One Correction

In the one-to-one correction scheme each quadrupole is used to move the beam into the centre of one BPM downstream. This is either the one in front of the next quadrupole or if one only uses focusing quadrupoles the one in front of the next focusing quadrupole.

For the one-to-one method using all quadrupoles the results are independent of the initial quadrupole positions—assuming infinitely precise BPMs. One finds $\Delta\epsilon_y \approx 840\,\%$ if only the nominal position errors and the BPM resolution are included. Figure 10 shows the emittance growth over the whole

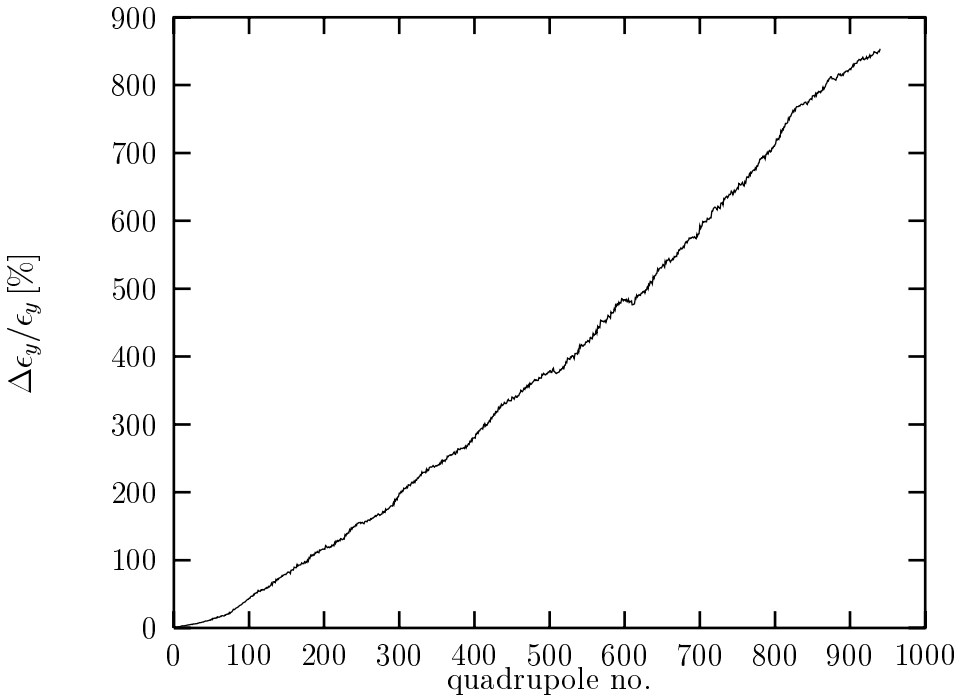

Figure 10: The emittance growth for the one-to-one correction scheme.

length of the linac. A possible error in the (mechanical) quadrupole movement does not contribute significantly to the emittance increase. The same is true for a small beam jitter during correction. Including a quadrupole movement error of $\sigma_M = 0.5\,\mu$m and an initial vertical jitter with an RMS of $\sigma_j = 0.1 \cdot \sigma_y$ one finds $\Delta\epsilon_y/\epsilon_y \approx 880\,\%$.

If one corrects only the focusing quadrupoles the result depends on the initial quadrupole position error. For initially perfectly aligned quadrupoles one finds $\Delta\epsilon_y/\epsilon_y \approx 320\,\%$. The dependence of the emittance growth on the quadrupole error is shown in Fig. 11. For $\sigma_{\rm quad} = 10\,\mu$m one finds $\Delta\epsilon_y/\epsilon_y \approx 420\,\%$.

With a BPM position error of $\sigma_{\rm BPM} = 2\,\mu$m the emittance growth is $\Delta\epsilon_y/\epsilon_y \approx 85\,\%$ for initially perfectly aligned quadrupoles and $\Delta\epsilon_y/\epsilon_y \approx 180\,\%$ for $\sigma_{\rm quad} = 10\,\mu$m. The beam jitter again has a very small effect leading to $\Delta\epsilon_y/\epsilon_y \approx 190\,\%$.

A non interleaved one-to-one correction leads for the same parameters to an emittance increase of about only 100 %.

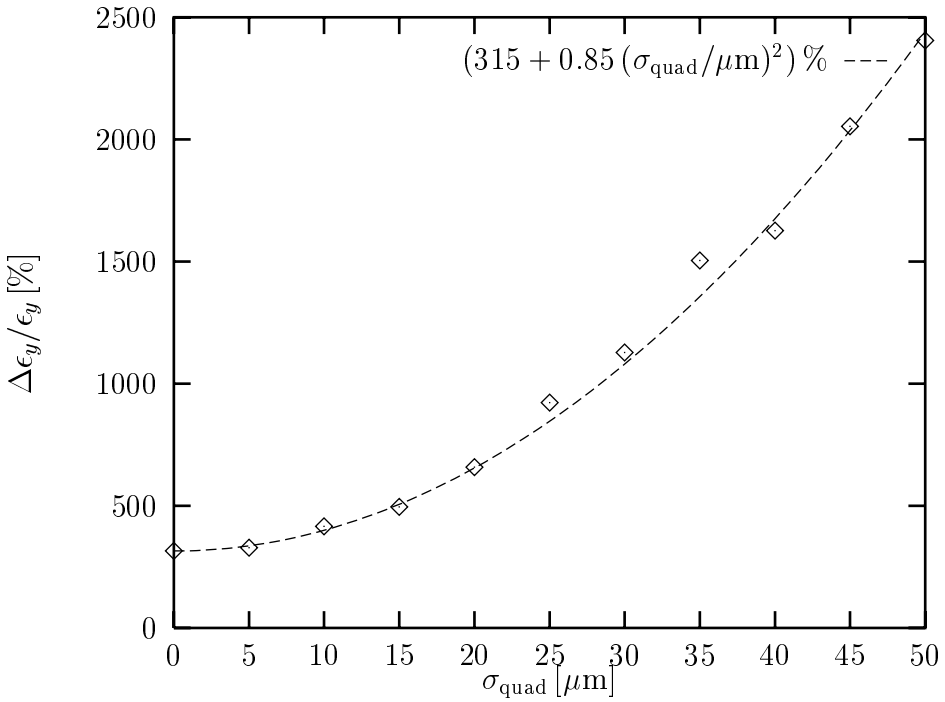

Figure 11: The emittance growth for the interleaved one-to-one correction scheme for different values of $\sigma_{\rm quad}$.

5.2 Ballistic Approach

The basic idea of the ballistic method is to align the BPMs first and the quadrupoles afterwards. This differs from the alignment method proposed for NLC [3] where the BPMs are positioned inside a quadrupole and are aligned to the quadrupole centres by varying their strength. In the ballistic method the correction is done bin-wise. In each bin all quadrupoles but the first are switched off. Its magnetic centre is moved to steer the beam through the centre of the last BPM of the bin. The centres of all the other BPMs in this bin are then moved onto the trajectory defined by the beam. This can be done either mechanically or by just introducing a calibration offset in the software. The quadrupoles are switched on—to their nominal settings—and a few-to-few correction of the bin is performed.

In the following each bin contains twelve quadrupoles. The emittance growth found for the nominal position errors and BPM resolution is about $\Delta\epsilon_y/\epsilon_y \approx 65\,\%$. In addition other error sources have to be considered, especially beam jitter during correction and remnant fields of the quadrupoles.

5.2.1 Beam Jitter

Beam jitter can in principle affect this method—especially during the ballistic step—since a small offset in the first quadrupole leads to a large offset in the last BPM. The measured value in this last BPM however needs not to be zero if the movement of the beam in the other BPMs due to the movement of the quadrupole is known. It is assumed that these response coefficients can be determined with an absolute error of $0.1\,\mu$m due to measurement precision and an additional relative error of one percent due to uncertainty of the shift of the quadrupole centre during the measurement. The latter is the same for all BPMs in a bin. With these assumptions the assumed beam jitter of $0.1\sigma_y$ at the entrance of the linac does not increase the emittance significantly.

5.2.2 Field Errors

The presents of field errors may be more severe. Two sources exist. The first are the deviations of the actual field strength from the selected if the quadrupole is switched on, the second are the presents of small remnant fields even if the quadrupole is switched off. The effect of the first can be reduced by iterating the correction with quadrupoles switched on until the BPM readings are zero. The second will affect the trajectory of the ballistic probe beam. Even if the remnant fields are small their effect can be large due to the large offsets of the quadrupoles. Iterating the complete correction can reduce this effect significantly as long as the procedure is stable, since in each step the quadrupole centres are moved closer to the beam trajectory thus reducing the kick due to the remnant fields.

The field errors at full quadrupole strengths are taken as normal distributed around the nominal value with a width of one per-mill of the nominal value. It is assumed that every time the quadrupoles are switched on this error is different. For the remnant fields it is assumed that it consists of a constant part that is different from quadrupole to quadrupole but the same each time the quadrupole is switched off. This part is modelled with a flat distribution ranging from zero to two percent of the maximal quadrupole strength. In addition there is a small random component taken to be a Gaussian with a width of one percent around the static value.

The effect of the iteration is illustrated in Fig. 12, where the offset of the centre-of-charge averaged over a hundred machines is shown. Without field errors the average deviation of the beam from the nominal axis is largest at the start and end of each bin. If field errors are included, the average deviation of the trajectory is largest in the centre of the bins while brought back close to the axis at the ends to go through the centres of the BPMs

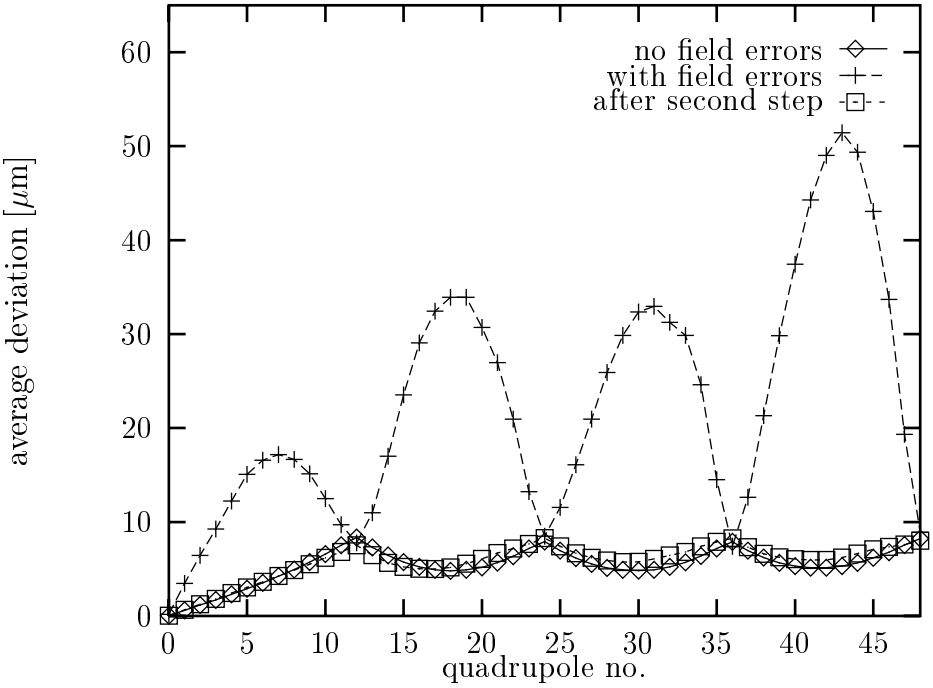

Figure 12: The average distance of the beam to the nominal axis in the first three correction bins.

there. While the amplitude seems to grow the maximal deviation averaged over the hundred cases does not exceed 60 μm along the linac. A second correction step essentially reproduces the behaviour of the case without field errors. The offset of the beam at the entrance of the linac was set to zero in these cases.

If the quadrupoles are switched off not only the field may be non zero but also their centres may be shifted compared to the full field strength. A normal distribution with a width of 10 μm was assumed for this shift which is different for each quadrupole but static. This resulted in virtually no change.

The beam jitter and field errors resulted in an average emittance increase of $\Delta\epsilon_y/\epsilon_y \approx 75\,\%$ which is very close to the 65 % found without them.

5.3 Emittance Bumps

The ballistic method can be combined with emittance bumps in order to further reduce the emittance growth. These consist in the following simulation of two accelerating structures that can be moved transversely followed by two quadrupoles used as a feedback to steer the beam onto its original trajectory. In practice the emittance bumps are optimised by the operator

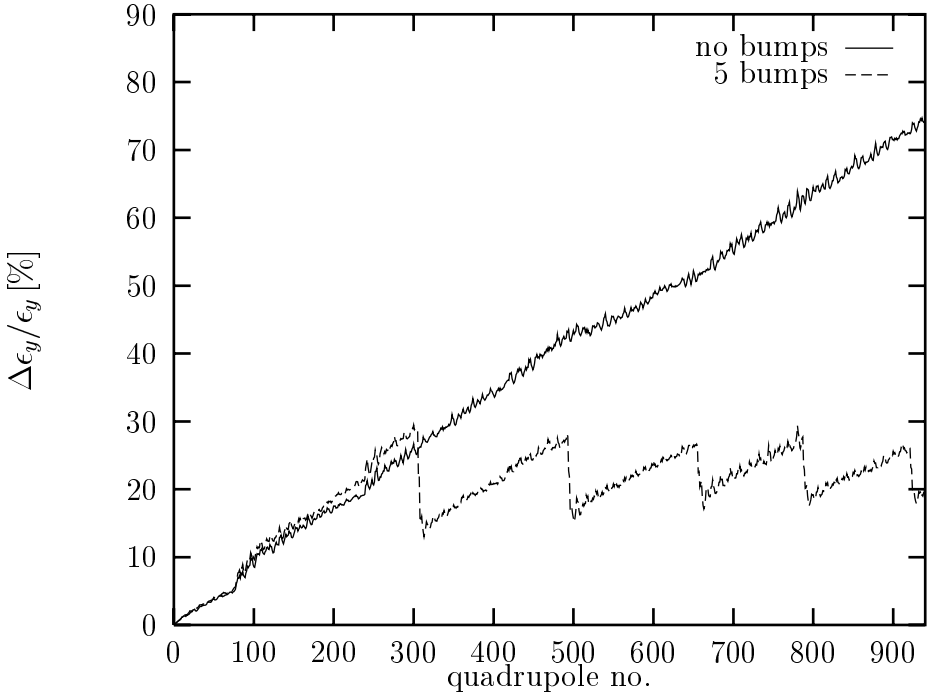

Figure 13: The average emittance growth including all error sources and five emittance bumps.

changing it in the two degrees of freedom and observing the emittance measured downstream. In the program a simple approximative approach is used that allows to determine the optimal setting directly.

The position of the bumps was not optimised, they where simply chosen to have equal distances. Using five bumps leads to $\Delta\epsilon_y \approx 20\,\%$, see Fig. 13. The probability distribution of $\Delta\epsilon_y$ is shown in Fig. 14. Of the one thousand simulated machines the simple ballistic correction gave a maximal vertical emittance growth of about 300 %, with an average of 75 %. Using five bumps reduced the average to 20 % and the maximum to less than 100 %.

5.4 Energy Spread

Up to this point the beam was assumed to have no initial energy spread. To achieve the required short bunchlength it is however necessary to compress the bunch before it enters the linac. This will enhance the energy spread the bunch has after leaving the damping ring roughly following

$$\Delta E_1 \sigma_{z,1} = \Delta E_2 \sigma_{z,2}$$

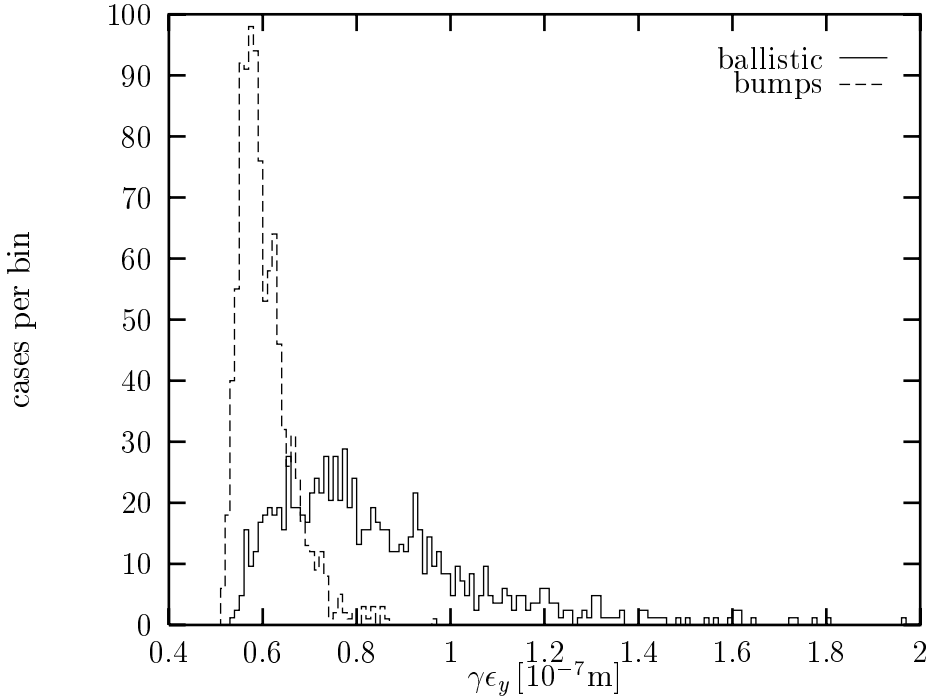

Figure 14: The probability distribution of the emittance growth using the ballistic method as well as applying five emittance bumps in addition. One thousand cases were simulated.

due to preservation of the longitudinal emittance. The energy spread is assumed to be Gaussian. Figure 15 shows the dependency of the emittance growth on the initial energy spread. The machines were corrected with the ballistic method and five bumps.

For the expected energy spread of 1.1 % [9] the effect is visible but small.

6 Ground Motion

The corrected linac will be affected by ground motion leading to a higher emittance increase after some time. In the following the ground motion is modeled using the so called ATL-law:

$$\Delta^2 = Atl \tag{5}$$

where Δ ist the relative position change of two points with a distance l after the time t. The constant A depends on the site of the linac an is usually assumed to be in the range from $0.5{\cdot}10^{-6}\,\mu\mathrm{m}^2/(\mathrm{ms})$[3] to $4{\cdot}10^{-6}\,\mu\mathrm{m}^2/(\mathrm{ms})$[7]. Here the first value is adopted. It should be noted that this model is a

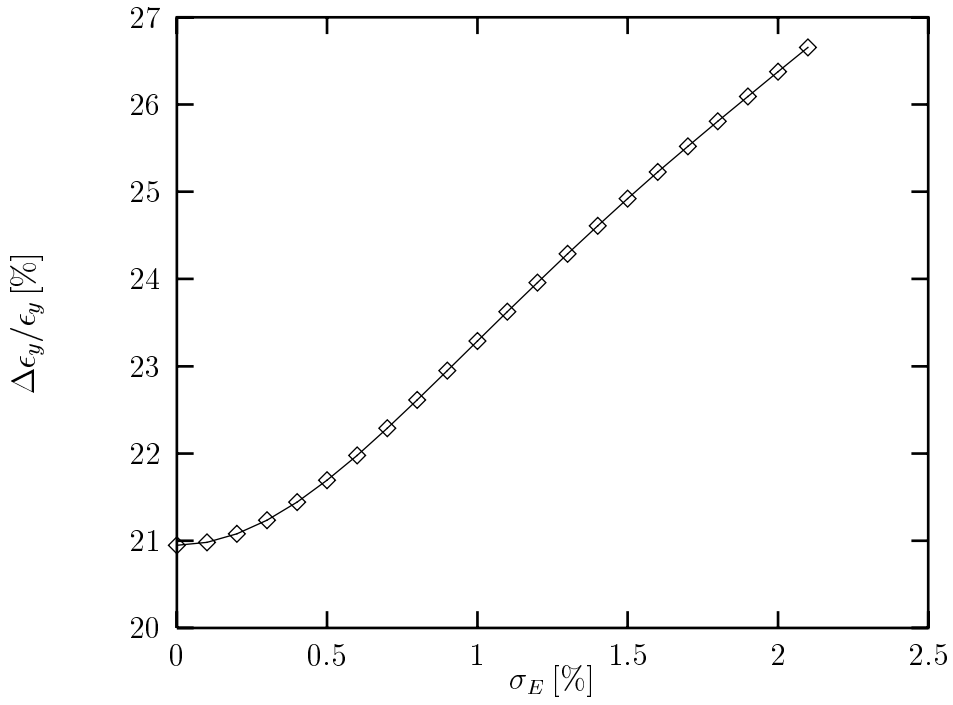

Figure 15: Dependence of the vertical emittance growth on the initial uncorrelated energy spread. The actual value will be around 1.1 %.

simplification to be able to give an upper estimate on the expected effect from ground motion. A more complete analysis would have to take correlations and specifics of the site into account. In the simulation the girders are moved according to the ATL-law, since the quadrupoles are not mounted directly onto them they could in principle move also with respect to the girder.

From the above law one expects the emittance growth to be linear with time, since the amplitudes scale with the square root of time and the emittance growth with the square of the amplitudes.

The effect of the ground motion on the emittance can be reduced by recorrecting the linac. Four steps of this correction seem usefull. The simplest is to use a small number of feedbacks to steer the beam onto its old trajectory at certain places. This can be done easily during normal operation. The next step is to use a simple one-to-one correction to steer the beam onto its old trajectory. This can also be done in feedback mode. In addition the emittance bumps can be reoptimised but this probably needs an operator doing it by hand so it can be done less frequently. The last step is to perform a full correction of the whole beamline.

To investigate the stability of the ballistic method a full correction is per-

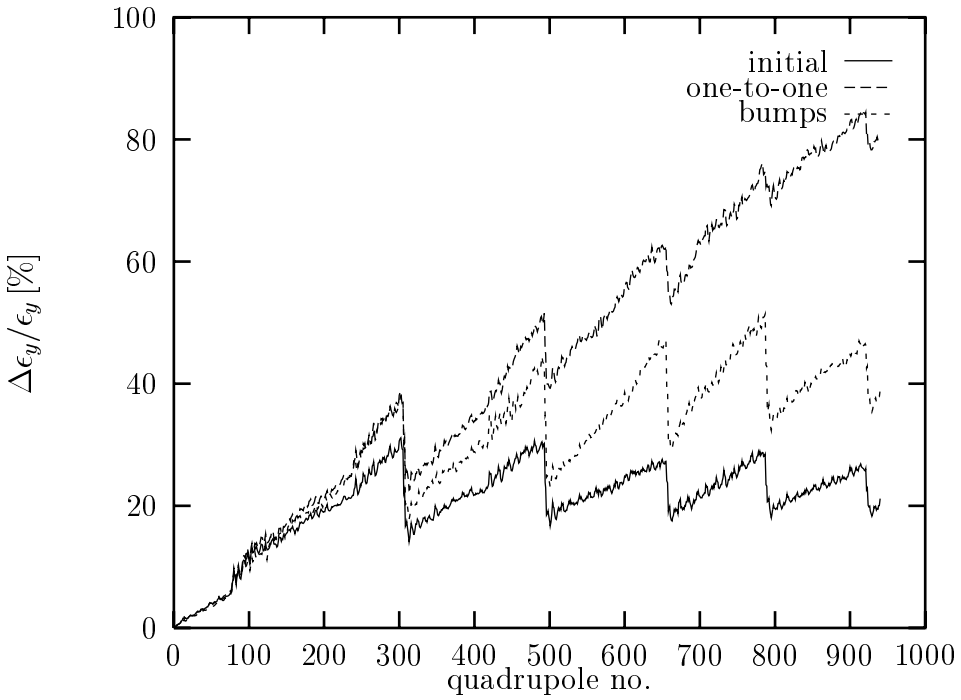

Figure 16: Emittance growth after $3 \cdot 10^6$ s with one-to-one correction and readjustment of the emittance bumps.

formed and the emittance growth to be expected after 3000 s—if no further correction is applied—is computed. The value found is $\Delta\epsilon_y/\epsilon_y \approx 400\,\%$; limiting the emittance growth to 6 % would thus require to repeat some correction more frequent than every minute. The simplest correction is the use the feedback stations already positioned at the emittance bumps. This leads to an increase of 200 % within 3000 s which is not an impressive improvement. More feedbacks can significantly improove the situation. Using the one-to-one correction in a feedback mode changes the performance significantly. After $3 \cdot 10^6$ s (about a month) later the emittance growth has increased by 60 %. Reoptimising the emittance bumps reduces this to only 20 %. Figure 16 shows the emittance growth imediately after the initial correction and after applying the two corrections.

One can thus expect the average time after which a full correction is again necessary to be of the order of weeks.

7 Multibunch Effects

In addition to the single bunch effects the multibunch wakefields are important. Besides the impact this has on the design of the cavities this also may affect the BPM design significantly, since it would be advantageous to be able to measure the bunch train. The simplest form is to take the centre of charge of the whole train, more refined designs might be able to resolve groups of bunches if not individual ones.

7.1 Longrange Wakefield Model

Since currently no detailed calculations of the longrange wakefields are available a simplified approach had to be chosen. It was assumed that the wakefield kick induced by a bunch onto another one could be calculated as

$$W_\perp(m-n) = w_1 W_{\perp,0} \exp\left(-a\,(m-n)\right) \tag{6}$$

where $w_1 W_{\perp,0}$ is the transverse wakefield amplitude at the second bunch and a a damping constant. $W_{\perp,0} = 1000\,\mathrm{kV/(pCm^2)}$ was assumed. Equation (6) implies that the phase of the wakefield is the same at all bunches. It is further assumed that the amplitude does not change over the length of bunches, so the created amplitude is just depending on the transverse position of the centre of charge of the driving bunch and is the same for all particles in the kicked bunch.

7.2 Results

The dependence of the allowed amplitude at the second bunch on the damping factor is illustrated in Fig. 17. A single machine was simulated and corrected using the ballistic method and emittance bumps. The emittance of a beam with 60 bunches passing through the machine was calculated for different values $w_1 W_{\perp,0}$ and a. The importance of the damping is obvious, with no damping even fields on the permille level at the second bunch lead to drastic emittance growth—while for strong damping (leading to a daisy-chain situation) rather large amplitudes can be accepted.

The emittance along the linac for different damping values a is shown in Fig. 18. The average of a sample of 30 machines is shown, where the correction was done using single bunch beams. While a value $a = 0.17$ leads to emittance growths that are much to high, the cases with $a = 0.22$ and $a = 0.27$ lead to less than 100 % emittance growth on average.

An example of the multibunch effects for a damping with $a = 0.27$ is given in Fig. 19 where the single bunch emittance (averaged over 20 machines) is

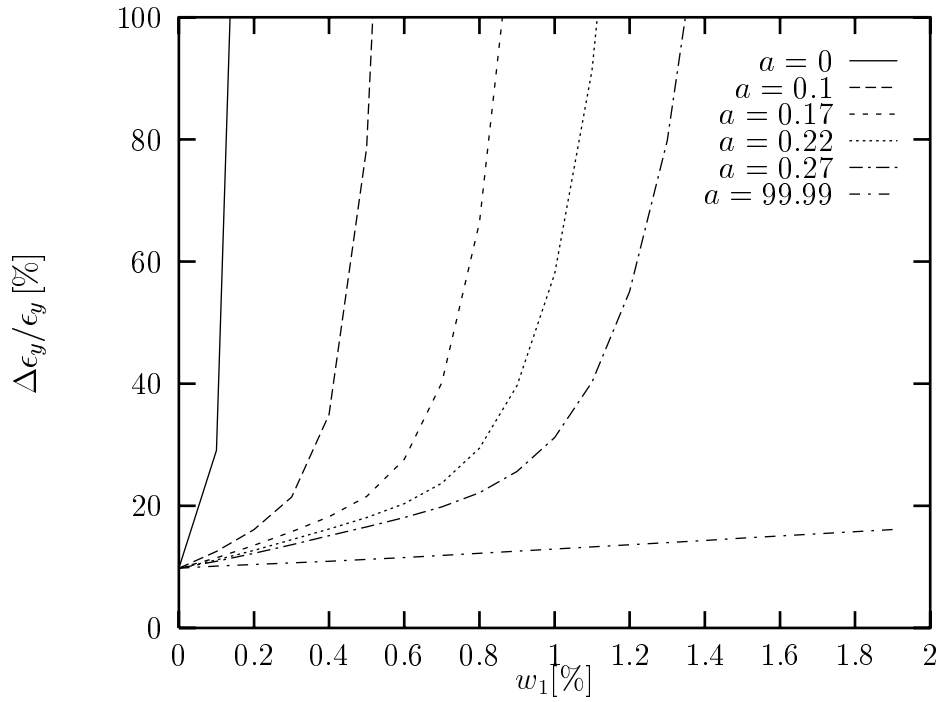

Figure 17: The dependence of the emittance growth on the wakefield amplitude at the second bunch for different dampings.

shown for all bunches. In the first case all correction steps are done using only a single bunch while in the second after the ballistic correction the bunch train is used for calibrating the emittance bumps and doing a one-to-one correction. In the first case the resulting emittance growth is significant, while it is strongly reduced in the second. The multibunch emittance along the linac is shown in Fig. 20. If the position of the centre of charge of the whole bunch train can be performed the resulting emittance growth seems to be rather modest, despite the pessimistic model.

8 Conclusions

In this paper a lattice for the CLIC main linac at 1 TeV centre-of-mass energy was presented together with a correction method that can achieve the required emittance growth of less than 100 %. The expected growth is around 70 % and can—with the help of five emittance bumps—be reduced to about 20 %. The proposed method should be robust and straightforward to implement on a real machine.

The linac is expected to be stable despite ground motion if one uses a

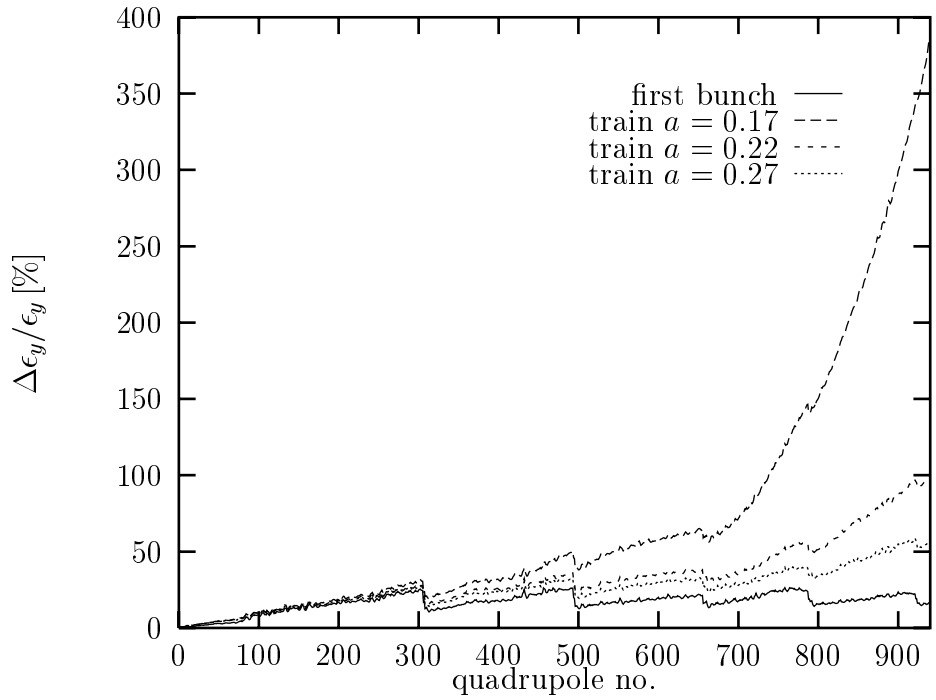

Figure 18: The multi bunch emittance growth along the linac for different values of the damping constant a. The beamline was corrected using a single bunch beam.

feedback based on a continuous one-to-one correction. A complete recorrection seems to be necessary at the timescale of weeks.

Further investigations of the ballistic method seem to be necessary to find its dependencies on the different error sources. The prealignment errors need to be modelled in a more precise manor especially reflecting the fact that the recovery after some time of ground motion is not perfect. The main linac lattice has to be optimised for a better fill factor and an even smaller emittance growth.

The multibunch effects need to be studied in detail using a less rough model.

9 Acknowledgement

The author would like to thank Tor Raubenheimer for numerous very usefull discussions.

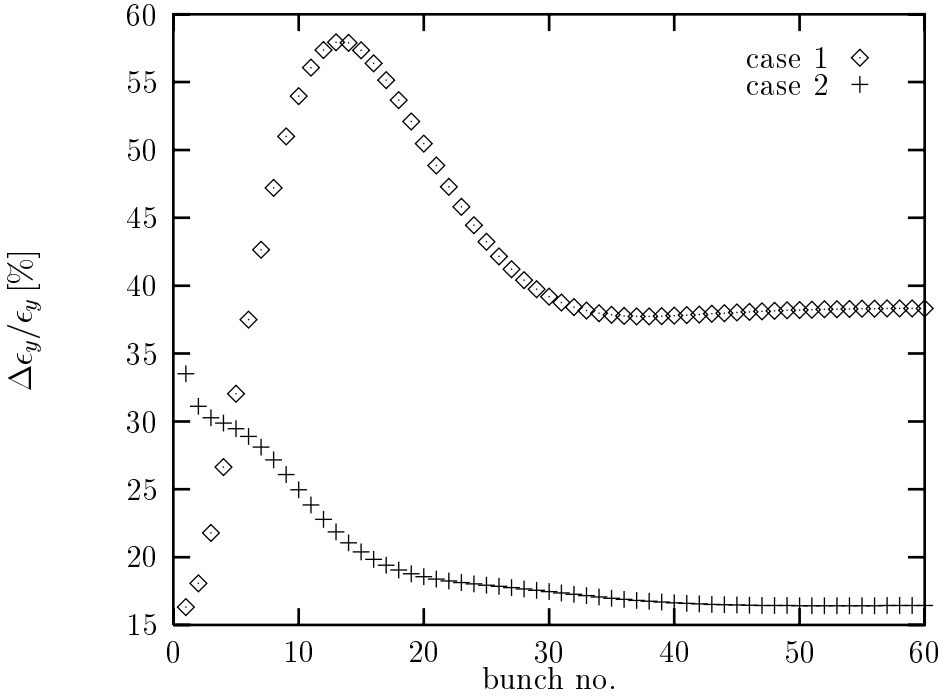

Figure 19: The final single bunch emittance of the bunches. In case 1 the alignment is done with single bunches only, while in case 2 the emittance bumps have been calibrated with the bunch train.

References

[1] V. Balakin, A. Novakhatsky, and V. Smirnow. In *12th Int. Conf. on High Energy Accelerators*, 1983.

[2] S. Farthouk. A statistical approach to analyse the efficiency of BNS damping and correction algorithms in linear colliders. *CLIC-Note 323.*

[3] The NLC Design Group. *Zeroth-Order Design Report for the Next Linear Collider.* 1996.

[4] Helene Mainaud. *Une nouvelle approche métrologique: L'écartométrie biaxiale. Application a l'alignment des accelerateur linéaires.* PhD thesis, Universite Louis Pasteur, Strasbourg, 1996.

[5] A. Millich. Computations of wakefields for CLIC DLWG. *CLIC-Note-137*, 1991.

[6] G. Parisi. Arrangement in sectors of CLIC main linac focusing. *CLIC-Note-221*, 1994.

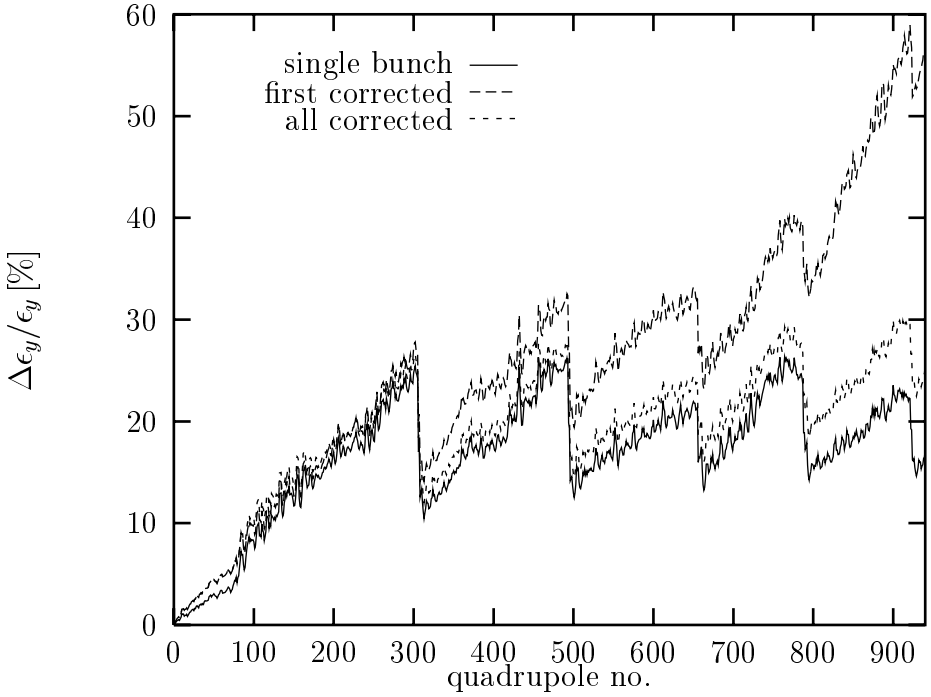

Figure 20: The emittance growth for single and multibunch cases. The beamline was corrected—using the ballistic method and five bumps—for a single bunch beam.

[7] J. Rossbach R. Brinkmann. Observation of closed orbit drift at HERA covering 8 decades of frequency. *Nucl. Instr. Meth. A*, 350 8-12, 1994.

[8] T. Raubenheimer. Private Communication.

[9] L. Rinolfi. Private communication.

[10] D. Schulte. To be published.

[11] R. Siemann. *SLAC-PUB-6417.*

[12] J. P. H. Sladen, I. Wilson, and W. Wünsch. CLIC beam position monitor tests. *CERN/PS-96-029-LP.*